

# PHYSICAL REVIEW C

## NUCLEAR PHYSICS

THIRD SERIES, VOLUME 35, NUMBER 5

MAY 1987

### 36-MeV-triton-induced charge exchange: Mass measurements and energy levels of neutron-rich nuclei and the charge exchange reaction mechanism

K. I. Pearce, N. M. Clarke, R. J. Griffiths, P. J. Simmonds,\* and A. C. Dodd  
*Wheatstone Laboratory, King's College London, Strand, London, United Kingdom*

D. Barker, J. B. A. England, M. C. Mannion, and C. A. Ogilvie  
*University of Birmingham, Birmingham, United Kingdom*

(Received 17 October 1986)

Energy spectra and differential cross sections have been obtained for the charge exchange reaction ( ${}^3\text{H}, {}^3\text{He}$ ) on targets of  ${}^{30,28}\text{Si}$  and  ${}^{26}\text{Mg}$  at an incident energy of 36 MeV. Previously unobserved energy levels of  ${}^{30}\text{Al}$  and  ${}^{26}\text{Na}$  are reported and compared to shell model predictions. Microscopic form factors based on the M3Y effective nucleon-nucleon interaction are used in distorted-wave Born approximation codes to fit the data. The sensitivity of the model to input parameters is discussed and some spin assignments made. Coupled channels calculations are performed to fit the two-step contributions to the data via sequential one-nucleon transfers.

#### INTRODUCTION

The ( ${}^3\text{H}, {}^3\text{He}$ ) reaction has been used to investigate the energy levels and masses of neutron rich nuclei.<sup>1-4</sup> In some cases these nuclei have only been observed by charge exchange reactions and the available data are sparse. For  ${}^{30}\text{Al}$  only five energy levels are mentioned in the literature,<sup>1,5,6</sup> of which only two have been confidently assigned spin-parity values (Fig. 2). For  ${}^{26}\text{Na}$ , 23 energy levels with  $E_x < 5.0$  MeV have been observed<sup>7</sup> using the  ${}^{26}\text{Mg}({}^3\text{H}, {}^3\text{He}){}^{26}\text{Na}$  reaction at 17 MeV, but limited data and lack of understanding of the charge exchange reaction mechanism has prevented assignment of any spin-parity values for the excited states. Attempts are now being made to understand the charge exchange reaction mechanism and to use it as a spectroscopic tool.

Investigations of the ( ${}^7\text{Li}, {}^7\text{Be}$ ) charge exchange reaction<sup>8-11</sup> have shown the importance of the tensor components of the effective nucleon-nucleon interaction to the direct process. Use of the central components alone tends to produce an oscillatory prediction not in agreement with the data. Inclusion of the tensor components damps the oscillations, producing better agreement between the shape of the prediction and the data. However, this model still fails to predict the correct magnitude for the cross sections.

Flynn *et al.*<sup>12</sup> reporting on  $1^+$  states excited by the reaction  ${}^{28}\text{Si}({}^3\text{H}, {}^3\text{He}){}^{28}\text{Al}$  at 17 MeV show that similarities exist between the strength distributions of electromagnetic excitation and charge exchange excitation. This provides strong evidence for the existence of the isospin mode with  $\Delta T = \pm 1$  of the collective  $M1$  vibration. A close similarity

between the two reaction mechanisms is implied.

Ajzenberg-Selove *et al.*<sup>13</sup> reporting on the ( ${}^3\text{H}, {}^3\text{He}$ ) reaction on targets of  ${}^{54,56,58}\text{Fe}$  and  ${}^{58}\text{Ni}$  at 25 MeV claim that the two step process ( ${}^3\text{H}, {}^4\text{He}$ )( ${}^4\text{He}, {}^3\text{He}$ ) adds considerably to the magnitude of the predicted cross sections, but does not significantly modify its angular shape. A later paper<sup>14</sup> extends this work to targets of  ${}^{40,42,44}\text{Ca}$ ,  ${}^{46,48,50}\text{Ti}$ ,  ${}^{54}\text{Cr}$ , and  ${}^{54}\text{Fe}$  and gives the same conclusion.

In order to further investigate the charge exchange reaction ( ${}^3\text{H}, {}^3\text{He}$ ), data were taken using the Nuclear Structure Facility's 20 MV tandem Van de Graaff accelerator to provide a 36 MeV beam of tritons. It was expected that this higher incident energy (the highest energy triton beam ever used at that time) would raise the cross sections of the reaction, making the measuring of good angular distributions possible.

#### EXPERIMENT

A Middleton-type sputter source,<sup>15</sup> in which absorbed tritium is liberated from a titanium cone by a cesium beam, was used to produce  ${}^3\text{H}^-$  ions. These were accelerated to 36 MeV by the tandem Van de Graaff accelerator.<sup>16</sup> Beam intensities of up to 600 nA on target were obtained, although the average beam current was about 200 nA.

The targets used were self-supporting foils of  ${}^{26}\text{Mg}$  (0.200 mg/cm<sup>2</sup> and 1.50 mg/cm<sup>2</sup>),  ${}^{30}\text{Si}$  (0.057 mg/cm<sup>2</sup>), and  ${}^{28}\text{Si}$  (0.130 mg/cm<sup>2</sup>). The target thicknesses were measured by 25 MeV alpha scattering experiments and confirmed by forward angle elastic scattering optical model searches. The thin  ${}^{30}\text{Si}$  target had small amounts

of  $^{16}\text{O}$  and  $^{12}\text{C}$  impurities which remained constant to within 5% throughout the experiment and allowed angular distributions to be obtained for these nuclei.

The Daresbury 1 m scattering chamber<sup>17</sup> was used with five  $\Delta E \cdot E$  semiconductor telescopes mounted on each of two independently rotating arms. The scattering angle could be set between  $7.5^\circ$  and  $170^\circ$  with an accuracy of better than  $1'$ . The  $\Delta E$  detectors were between 118 and  $155 \mu\text{m}$  thick with  $E$  detectors being 5 mm thick. These were cooled to improve energy resolution.

Mass and energy signals were produced by Daresbury particle identifiers,<sup>18</sup> digitized and sorted in hardware. This allowed very fast data acquisition rates (up to 2 kHz on any telescope or 10 kHz overall). Data were collected for the five ejectiles  $^1,2,3\text{H}$ ,  $^3,4\text{He}$ .

Analyses of the elastic scattering, inelastic scattering, and one-nucleon transfer data have been presented elsewhere.<sup>19,20,21</sup>

Differential cross sections were obtained for the charge exchange reaction over the angular ranges  $15^\circ < \theta < 55^\circ$  for  $^{30}\text{Si}$  targets,  $15^\circ < \theta < 50^\circ$  for  $^{26}\text{Mg}$  targets, and  $15^\circ < \theta < 35^\circ$  for  $^{28}\text{Si}$  targets. Figure 1 shows a sample energy spectrum for the  $^{30}\text{Si}(^3\text{H}, ^3\text{He})^{30}\text{Al}$  reaction.

#### ENERGY LEVELS OF $^{30}\text{Al}$

Energy spectra of  $^{30}\text{Al}$  were obtained over the angular range  $15^\circ < \theta < 55^\circ$  with  $1.25^\circ$  ( $2.5^\circ$ ) spacing at forward (backward) angles. Peaks caused by the presence of  $^{12}\text{C}$ ,  $^{16}\text{O}$ , and  $^{28}\text{Si}$  impurities in the target provided between seven and fifteen calibration points above, below, and interspaced with the  $^{30}\text{Al}$  levels, allowing good calibration of these spectra. This calibration assumed a linear relationship between channel number and energy, used relativistic kinematics, and made allowances for energy losses in the target.

The estimated errors in the individual measurements of the peak energies ranged from 11 to 15 keV depending on the quality of the calibration and the definition of the peaks. The standard deviations of the values from different angles ranged from 11 to 30 keV with 15 keV as the

modal value. The relative inaccuracy of some of the measurements may be the result of their being multiplet states or being seen at fewer angles due to their weakness or to their being covered by contaminant peaks at some angles.

Errors in the measurement of  $Q$  values by this method may be caused by errors in the measurement of the ejectile angle, errors in the energy of the incident beam, target energy losses, and nonlinearities in the detectors and associated electronics.

The latter is known to be a very small effect since the calibration points were seen to be very linear and extended above and below the region of interest. The energy resolution of the beam was expected to be of the order of 1 in  $10^4$ , with the actual beam delivered expected to be within 1 in  $10^3$  of the requested value. The energy spread corresponds to 3.6 keV, small compared to the spread of the results, and its treatment is inherent in the analysis. The effect of any offset in the actual beam energy delivered would also be small since the calibration depends more on the relative position of the peaks than their absolute position. The angular positions of the detectors were measured to within a few minutes of arc. This, and the angular acceptance of the detectors, only contribute a fraction of a keV to any errors in the analysis. Thus it seems reasonable to use the spread of the results as the error measurement when quoting excitation energies of the newly measured levels. The possible systematic errors that have been considered all lead to very small additional errors.

The ground state  $Q$  value for the reaction  $^{30}\text{Si}(^3\text{H}, ^3\text{He})^{30}\text{Al}$  was measured to be  $-8.545 \pm 0.015$  MeV compared to the previous best measurement of  $-8.52 \pm 0.04$  MeV. Using the mass excesses quoted in Ref. 22, this gives a value of  $-15868.1 \pm 15$  keV for the mass excess ( $M - A$ ) of  $^{30}\text{Al}$  and  $29.98296 \pm 0.000016$  MeV/nucleon for its mass.

The energy levels of  $^{30}\text{Al}$  measured in this way are shown in Table I, where they are compared with previously published<sup>1,5,6</sup> and unpublished<sup>10</sup> measurements; the yields (based on 100 for the ground state) are given, where

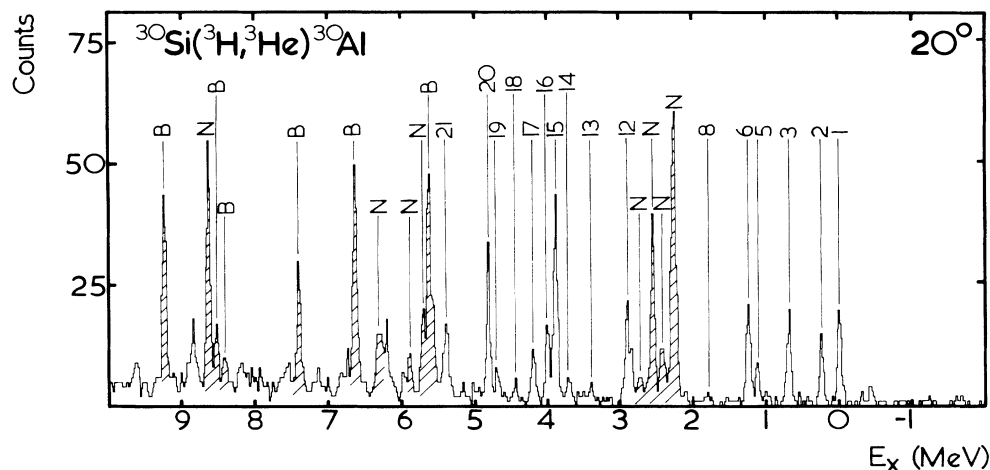


FIG. 1. Energy spectra for the reaction  $^{30}\text{Si}(^3\text{H}, ^3\text{He})^{30}\text{Al}$ . The numbers correspond to excitation energies listed in Table I. The shaded peaks are due to known target contaminants and are labeled by the chemical symbol of the residual.

TABLE I. Excitation energies (in keV) of all levels (number in parentheses is error in least significant figure) and yields (g.s.=100) at 14° and 44° where available.

| Level No. | Kozub <i>et al.</i> | $({}^7\text{Li}, {}^7\text{Be})$<br>Dodd | $({}^3\text{H}, {}^3\text{He})$<br>This work | Yield  |        |
|-----------|---------------------|--|--|--------|--------|
|           |                     |  |  | 14°    | 44°    |
| 1         | 0.0                 | 0.0                                      | 0.0  | 100.00 | 100.00 |
| 2         | 243.90(8)           | 252(4)                                   | 245(17)                                      | 229.87 | 358.92 |
| 3         | 687.5               | 701(10)                                  | 694(15)                                      | 121.66 | 159.37 |
| 4         | 991.0(9)            |  |  |        |        |
| 5         | 1119                | 1112(16)                                 | 1120(23)                                     | 19.50  | 67.92  |
| 6         | 1245.6(8)           | 1263(18)                                 | 1253(11)                                     | 68.91  | 203.67 |
| 7         |                     | 1554(22)                                 |  |        |        |
| 8         |                     | 1717(24)                                 | 1822(17)                                     | 24.44  | 42.78  |
| 9         |                     | 2322(33)                                 | 2303(15)                                     |        | 137.79 |
| 10        |                     | 2455(35)                                 | 2454(20)                                     | 74.91  | 70.22  |
| 11        |                     | 2738(39)                                 | 2744(15)                                     | 117.46 | 77.01  |
| 12        |                     | 2929(42)                                 | 2892(15)                                     | 132.87 | 240.50 |
| 13        |                     | 3396(48)                                 | 3461(30)                                     |        |        |
| 14        |                     |  | 3705(17)                                     | 39.30  |        |
| 15        |                     |  | 3908(17)                                     | 203.24 | 272.42 |
| 16        |                     |  | 4009(10)                                     | 150.95 | 131.38 |
| 17        |                     |  | 4201(19)                                     | 54.05  |        |
| 18        |                     |  | 4463(15)                                     | 9.09   |        |
| 19        |                     |  | 4694(15)                                     | 41.26  |        |
| 20        |                     |  | 4814(15)                                     |        | 167.64 |
| 21        |                     |  | 5415(15)                                     | 76.86  |        |
| 22        |                     |  | 5553(15)                                     | 51.46  |        |
| 23        |                     |  | 5901(19)                                     |        | 61.03  |

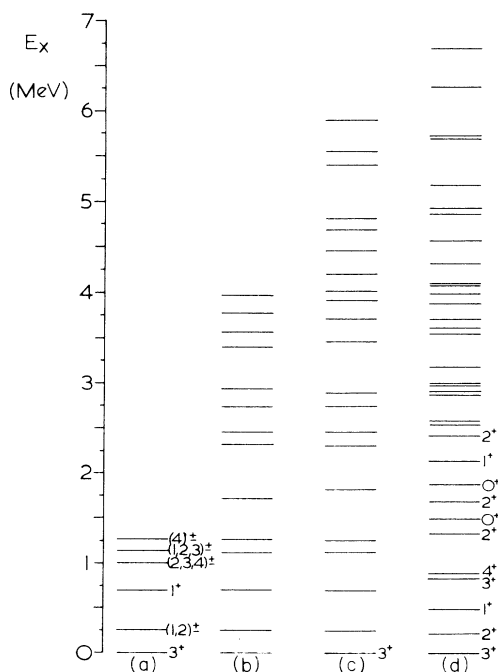


FIG. 2. Energy levels of  ${}^{30}\text{Al}$ . (a) Published, (b) Dodd, (c) present, and (d) shell model.

available, at 14° and 44°. These energy levels are shown schematically in Fig. 2, together with levels obtained using the  $({}^7\text{Li}, {}^7\text{Be})$  reaction at 72 MeV.<sup>10</sup>

The 1 MeV level tentatively proposed by Ajzenberg-Selove *et al.*<sup>1</sup> and assigned an excitation of  $991.0 \pm 0.9$  keV by Kozub *et al.*<sup>6</sup> was not observed either by Dodd<sup>10</sup> or in the present work. It must be concluded that this level is only very weakly excited by charge exchange or that it does not exist.

The final column in Fig. 2 shows shell model predictions of the energy levels of  ${}^{30}\text{Al}$ . These predictions are based on the  $A$ -dependent interactions of Wildenthal.<sup>23</sup> In these calculations the two body matrix element magnitudes decrease with  $A$  as  $(18/A)^{0.3}$  in an attempt to describe the entire  $2s-1d$  shell in a self-consistent manner. At first sight, it seems that the agreement between our results and the shell model prediction is not very good compared to the agreements that can be obtained from this model. However, having many active orbitals,  ${}^{30}\text{Al}$  is a severe test of shell model calculations. It does seem that the first five energy levels predicted correspond to the first five measured levels; their relative separations agree closely, but the predicted excitation energies are too low. It is likely that some of the levels found in this work correspond to more than one energy level since the average level spacing of similar nuclei is about 40 keV per level and the experimental resolution was only 70 keV. Another feature to consider is the possible selectivity of the charge exchange reaction. That is, it is possible that ener-

gy levels exist in  $^{30}\text{Al}$  that are not excited by the reaction or are too weakly excited to be seen above the background in the spectra. However, the energy spectra obtained from the reaction  $^{28}\text{Si}(^3\text{H}, ^3\text{He})^{28}\text{Al}$  showed a large number of excited states with no known level obviously missing within the limitations of the resolution.

#### ENERGY LEVELS OF $^{26}\text{Na}$ LEVELS

Energy spectra were obtained for  $^{26}\text{Na}$  over the angular range  $15^\circ < \theta < 50^\circ$ . Since these spectra were relatively free of impurity peaks and the level structure of  $^{26}\text{Na}$  is better known,<sup>7</sup> the calibration was performed using the known levels of  $^{26}\text{Na}$  as reference points. Previously unreported levels of  $^{26}\text{Na}$  were observed at  $4.97 \pm 0.04$  and  $5.08 \pm 0.06$  MeV with evidence of a level at  $1.86 \pm 0.06$  MeV and a group of levels between 1.45 and 1.65 MeV. Poor statistics at backward angles and the presence of  $^{16}\text{N}$  states at forward angles prevented more confident measurements of these lower excited states. (See Fig. 3).

#### CHARGE EXCHANGE CALCULATIONS

The microscopic theory of charge exchange has been reviewed in previous papers<sup>8,11</sup> and will not be presented in detail here.

The charge exchange process is treated as inelastic scattering, involving changes in the spin and isospin of both the projectiles and target nuclei, but not their mass number. The interaction potential is assumed to be the

sum of an effective two-body nucleon-nucleon interaction over the nucleons in the projectile and target. The important terms of the interaction are considered to be the central and tensor terms with the spin-orbit interaction producing a negligible contribution to the cross sections.

The double folding code CHEX2 (Ref. 24) was used to generate the direct charge exchange form factors using the Bertsch M3Y effective nucleon-nucleon interaction.

The explicit form of the interaction used was

$$V_{01}^0(s) = -4886e^{-4s}/4s + 1175e^{-2.5s}/2.5s + 310\delta(s),$$

$$V_{11}^0(s) = -421e^{-4s}/4s + 480e^{-2.5s}/2.5s \\ + 3.5e^{-0.7s}/0.7s - 145\delta(s),$$

$$V_{11}^2(s) = 386s^2e^{-2.5s}/2.5s + 10.5s^2e^{-1.43s}/1.43s.$$

In common with the work of Dodd *et al.*,<sup>11</sup> Woods-Saxon wave functions were used to describe the bound states. These used a radius parameter of  $1.25A^{1/3}$  fm and a diffuseness parameter of 0.65 fm; the depth was calculated to fit the separation energy. Previous works have used harmonic oscillator wave functions rather than Woods-Saxon ones, but it has been shown that there is generally good agreement between the results. The spectroscopic amplitudes were calculated assuming pure particle-hole configurations.

Figure 4 shows the form factors obtained from CHEX2 for the  $3^+$  ground state in the reaction  $^{30}\text{Si}(^3\text{H}, ^3\text{He})^{30}\text{Al}$ . The two possible combinations of  $lsj$  transfer that are possible (213, 413) are calculated separately and repeated for central terms alone ( $C$ ), tensor terms alone ( $T$ ), and central and tensor terms combined ( $C+T$ ).

Figure 5 shows the cross section predictions that are obtained from distorted-wave Born approximation (DWBA) calculations using this type of form factor in the King's College version of CHUCK3.<sup>25</sup> The optical potentials used in these calculations were based on the parameters found in the analysis of the elastic scattering data measured during the experiment<sup>19</sup> for the entrance channel and 33.2 MeV helion parameters from the literature for the exit channel. These parameters and their references are given in Table II. These calculations are performed in the zero range approximation. Calculations are presented for  $1^+$ ,  $2^+$ ,  $3^+$ , and  $4^+$  states in  $^{30}\text{Al}$ , assuming a  $pd_{5/2} \times nd_{3/2}$  configuration, and the  $C$ ,  $T$ , and  $C+T$  contributions are all shown. As shown by Dodd *et al.*,<sup>11</sup> for the  $1^+$  and  $3^+$  cases the central and tensor terms each produce oscillato-

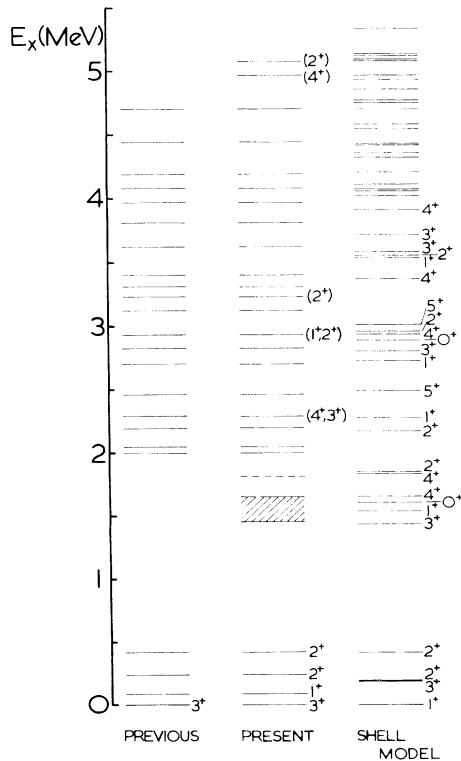


FIG. 3. Energy levels of  $^{26}\text{Na}$ : published, present, and shell model.

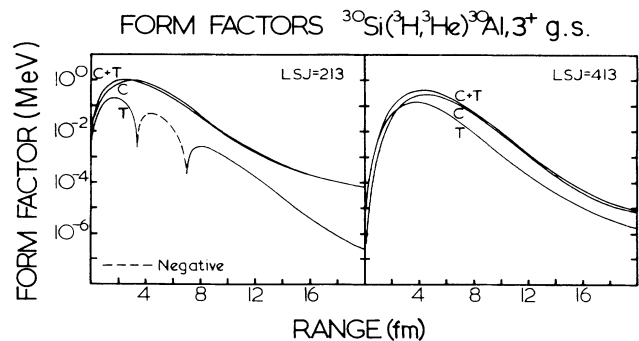


FIG. 4. Charge exchange form factors.

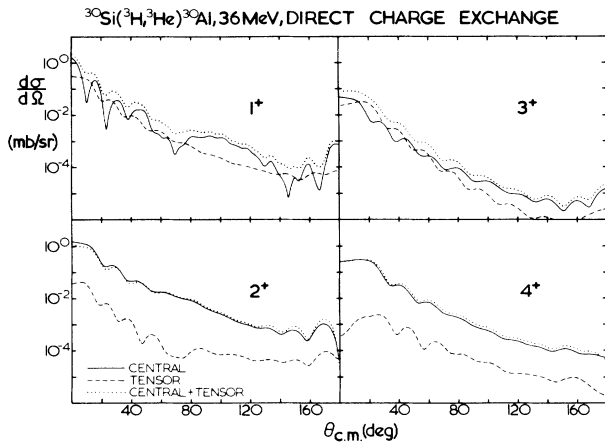


FIG. 5. Direct charge exchange cross section predictions.

ry cross sections of about equal magnitude but out of phase. The combination of the two terms produces relatively structureless angular distributions in better agreement with the data.

An investigation of the sensitivity of these calculations to some of the input parameters was performed. It was found that the use of deeper entrance and exit optical model parameters ( $J_r \sim 500 \text{ MeV fm}^3$ ) enhanced the cross sections by a factor of about 2 without changing the shape of the distribution very much. The results seemed insensitive to the form of the imaginary potential (volume or surface) used. Changing the bound state geometry parameters by up to 10% for all the states also led to factors of up to two differences in the cross section predictions. However, if steps were made to preserve the rms radii of the bound states by increasing the radius while decreasing the diffuseness parameter and vice versa, the effect was very much smaller as found by Dodd *et al.*<sup>11</sup>

It was seen that including the effects of excitation of

the residual nucleus in the calculation of the form factor had a small effect ( $< 20\%$  for 3 MeV excitation). These calculations are complicated by uncertainty as to how the effects should be included in the calculations, but all reasonable methods proved equally insensitive. The inclusion of excitation in the generation of the distorted waves was seen to be a greater effect than its inclusion in the form factor calculation. The result of increasing excitation being a reduction in cross section and a damping out of angular structure. Because of this it was decided to adopt the usual practice of using ground state form factors for the excited states but to generate the distorted waves correctly.

#### MICROSCOPIC CHARGE EXCHANGE FITS TO $^{30}\text{Si}(^3\text{H}, ^3\text{He})^{30}\text{Al}$ DATA

Figure 6 shows how the direct charge exchange predictions compare to the data. The predictions for the ground state (known to be a  $3^+$ ) slightly underestimate the data and fail to fit the oscillations beyond  $30^\circ$  particularly well. This is typical of the  $3^+$  ground states observed in these experiments. Two possible shell model configurations of the  $3^+$  ground state are considered:  $pd_{5/2}^{-1} \times nd_{3/2}$  and  $pd_{5/2}^{-1} \times ns_{1/2}$ . Pure particle-hole spectroscopic amplitudes have been employed. In reality, some combination of these configurations would be expected.

The first excited state ( $E_x = 0.24 \text{ MeV}$ ) has been assigned a spin of either 1 or 2. These fit the first minimum and maximum quite well then fall off too rapidly with angle. Two step processes might be expected to enhance the backward angle cross sections.

The second excited state ( $E_x = 0.69 \text{ MeV}$ ) has been assigned a spin and parity of  $1^+$  and this is seen to fit the data quite successfully out to  $35^\circ$ . However, the  $2^+$  predictions also shown are at least as good as the  $1^+$  predictions at forward angles and beyond  $35^\circ$  are actually better than the  $1^+$ .

The third excited state ( $E_x = 1.12 \text{ MeV}$ ) has been as-

TABLE II. Optical model parameters used in calculations.

| Channel                        | $U_s$<br>(MeV) | $r_s$<br>(fm) | $a_s$<br>(fm) | $W_s$<br>(MeV) | $W_d$<br>(fm) | $R_i$<br>(fm) | $a_i$<br>(fm) | Ref. |
|--------------------------------|----------------|---------------|---------------|----------------|---------------|---------------|---------------|------|
| $^{30}\text{Si} + ^3\text{H}$  | 194.63         | 1.07          | 0.722         | 21.538         |               | 1.587         | 0.768         | 19   |
| $^{31}\text{Si} + ^2\text{H}$  | 79.27          | 1.17          | 0.648         | 1.62           | 11.52         | 1.325         | 0.75          | 28   |
| $^{29}\text{Al} + ^4\text{He}$ | 172.10         | 1.18          | 0.710         | 25.90          |               | 1.38          | 0.232         | 29   |
|                                |                |               |               |                | 5.56          | 1.31          | 0.745         |      |
| $^{30}\text{Al} + ^3\text{He}$ | 196.2          | 1.07          | 0.738         | 21.220         |               | 1.56          | 0.926         | 30   |
| $^{28}\text{Si} + ^3\text{H}$  | 145.0          | 1.14          | 0.739         | 21.254         |               | 1.627         | 0.745         | 19   |
| $^{29}\text{Si} + ^2\text{H}$  | 83.15          | 1.17          | 0.648         | 1.60           | 13.02         | 1.325         | 0.743         | 28   |
| $^{27}\text{Al} + ^4\text{He}$ | 172.10         | 1.18          | 0.710         | 25.90          |               | 1.38          | 0.232         | 29   |
|                                |                |               |               |                | 5.56          | 1.31          | 0.745         |      |
| $^{28}\text{Al} + ^3\text{He}$ | 145.0          | 1.14          | 0.739         | 21.254         |               | 1.627         | 0.745         | 19   |
| $^{26}\text{Mg} + ^3\text{H}$  | 171.37         | 1.16          | 0.670         | 27.382         |               | 1.511         | 0.819         | 19   |
| $^{27}\text{Mg} + ^2\text{H}$  | 82.66          | 1.17          | 0.770         | 1.5967         | 11.539        | 1.325         | 0.550         | 28   |
| $^{25}\text{Na} + ^4\text{He}$ | 172.10         | 1.18          | 0.710         | 25.90          |               | 1.38          | 0.745         |      |
|                                |                |               |               |                | 5.56          | 1.31          | 0.745         |      |
| $^{26}\text{Na} + ^3\text{He}$ | 178.72         | 1.118         | 0.662         | 38.124         |               | 1.292         | 0.986         | 31   |

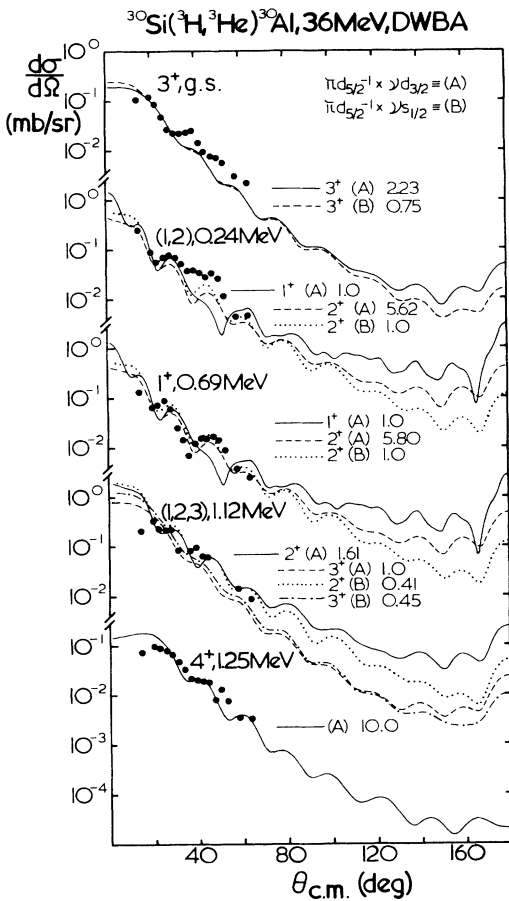


FIG. 6. Direct charge exchange fits for the reaction  $^{30}\text{Si}(^3\text{H},^3\text{He})^{30}\text{Al}$ .

signed a spin of 1, 2, or 3 with unknown parity. The data are insufficiently oscillatory to fit the  $1^+$  prediction at all, but somewhat more oscillatory than the  $3^+$  predictions. A very tentative assignment of  $2^+$  could be made with a note that the  $3^+$  possibility cannot positively be ruled out.

The fourth excited state ( $E_x = 1.25$  MeV) is quite well fitted as a  $4^+$ . However, this prediction has been normalized by a factor of 10 to reach the data.

MICROSCOPIC CHARGE EXCHANGE FITS  
TO  $^{28}\text{Si}(^3\text{H},^3\text{He})^{28}\text{Al}$

Data were obtained for several levels of  $^{28}\text{Al}$ , but few are single states, so assumptions have to be made about which state is dominant. Dodd *et al.*<sup>11</sup> investigated the reaction  $^{28}\text{Si}(^7\text{Li},^7\text{Be})^{28}\text{Al}$  at 72 MeV, and claimed that the dominant term in the  $3^+$  g.s./ $2^+$  0.03 MeV doublet is the  $3^+$  level. This was based on inspection of the spectra; with a resolution of 70 keV and a dispersion of 1 keV per channel, an edge was seen on the high energy side of the peak. This edge was thought to be the 0.03 MeV state and was estimated to be no more than 20% of the total peak. In the present experiment similar resolution was

achieved, but, with a dispersion of 30 keV per channel, no structure for the peak could be seen. Using Dodd's work as a guideline, we can assume that the first peak is mainly the  $3^+$  ground state. The second peak observed is an admixture of a  $3^+$  state at 1.01 MeV and a  $0^+$  state at 0.97 MeV. This is assumed to be mainly the  $3^+$  state because of the similarity between its angular distribution and that of the ground state. The third peak is a pure  $1^+$  state at 1.37 MeV, while the fourth is again an admixture, this time of a  $1^+$  state at 1.620 MeV and a  $2,3^+$  state at 1.622 MeV. This fourth state will be assumed to be a  $1^+$  state. No other positive parity states were extracted at sufficient angles to be worthy of analysis. The negative parity states will not be discussed in this paper.

Another question to consider is the shell model configurations of the extracted states. The  $1^+$  states are considered to be well described by the  $1d_{5/2}^{-1} \times 1d_{3/2}$  configurations, with the transition strengths being split over many energy levels by residual interactions. Thus the sum of all the  $1^+$  cross sections should about equal the pure  $d_{5/2}^{-1} \times d_{3/2}$  prediction if the M3Y interactions employed are of reasonable strength.

The  $2^+$  and  $3^+$  levels can be explained either as  $d_{5/2}^{-1} \times d_{3/2}$  or as  $d_{5/2}^{-1} \times 2s_{1/2}$  configurations and the level structure of  $^{28}\text{Al}$  can be explained by assuming that these levels are also split by residual interactions. Dodd *et al.* claim that the  $2^+$  strength is concentrated in the 3.94 MeV level (0.65) and the 3.35 MeV level (0.14), leading to the conclusion that the 0.03 MeV level must represent less than 21% of the  $2^+$  strength.

Figure 7 shows the direct charge exchange fits obtained for the first four extracted levels of  $^{28}\text{Al}$ . For the ground

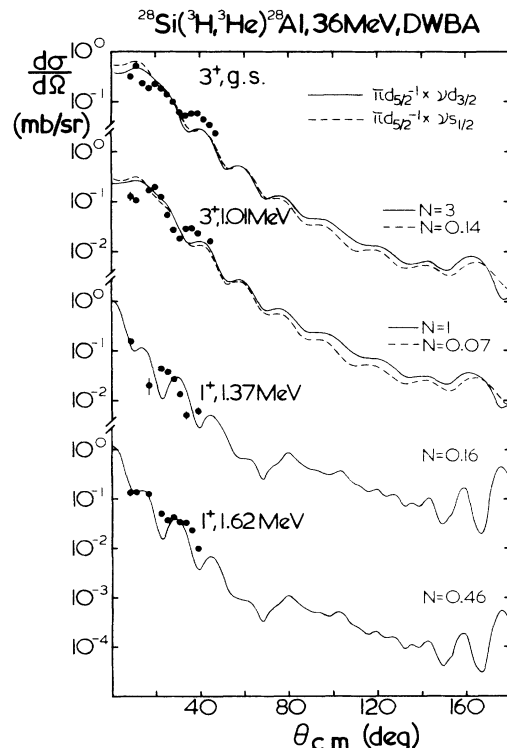


FIG. 7. Direct charge exchange fits for the reaction  $^{28}\text{Si}(^3\text{H},^3\text{He})^{28}\text{Al}$ .

state only the two  $3^+$  predictions are shown; the  $2^+$  predictions fall off too steeply and are too oscillatory. The fact that the  $3^+$  predictions are better and that the data look like those obtained for the ground states of  $^{26}\text{Na}$  and  $^{30}\text{Al}$  supports the assumption that the ground state is the dominant term in this doublet. In a similar manner to the  $^{26}\text{Na}$  and  $^{30}\text{Al}$  cases the first broad slope of the data is quite well fitted but the maximum beyond  $30^\circ$  is not fitted very well.

The first excited state at 1.01 MeV looks very similar to the ground state data, confirming that the  $0^+$  component of the data is relatively weak. Again, the forward angle fit is quite good, with the second maximum being under-predicted. The fit to the  $1^+$  state at 1.3 MeV is quite badly out of phase, but reproduces the shape of the distribution quite successfully. The data for the 1.62 MeV level are less oscillatory than the  $1^+$  prediction; this could be a result of the admixture of the  $2,3^+$  state filling in the minima.

The normalizations between the data and predictions for this work (Dodd *et al.*<sup>11</sup>) were, for the  $3^+$  ground state, 0.14(0.26), for the 1.01 MeV  $3^+$  state, 0.32(0.07), and for the 1.6 MeV  $1^+$  state, 0.2(0.07). Where the normalizations quoted for this work are those using the same shell model configurations as Dodd *et al.* ( $pd_{5/2}^{-1} \times nd_{3/2}$  for  $1^+$  states and  $pd_{5/2}^{-1} \times ns_{1/2}$  for  $3^+$ ).

It is, perhaps, cause for worry that the ( $^3\text{H}, ^3\text{He}$ ) investigation does not obtain the same normalization as the ( $^7\text{Li}, ^7\text{Be}$ ) investigation of Dodd *et al.*<sup>11</sup> This could be due to differences in the importance of two step processes which will be investigated in later sections.

#### MICROSCOPIC CHARGE EXCHANGE FITS TO $^{26}\text{Mg}(^3\text{H}, ^3\text{He})^{26}\text{Na}$

Data were obtained for many levels of  $^{26}\text{Na}$  excited by the reaction  $^{26}\text{Mg}(^3\text{H}, ^3\text{He})^{26}\text{Na}$ . The first four states in this nucleus are very closely packed, the fourth state being at an excitation of 0.42 MeV; because of this the counts for each level were obtained by fitting four Gaussians to the overall peak.

Figure 8 shows the direct charge exchange predictions to these low lying levels. For  $2^+$  and  $3^+$  states there are two possible shell model configurations to consider:  $pd_{5/2}^{-1} \times nd_{3/2}$  and  $pd_{5/2}^{-1} \times ns_{1/2}$ ; these give a similar shape of distribution but differ in magnitude by a factor of about 10. The normalizations between the data and predictions are shown on the figure.

The ground state is predicted to be a  $1^+$  state, but has been experimentally assigned as a  $3^+$ . Of the three possibilities, the  $1^+$  prediction produces the worst fit to the forward angle data. The data look very similar to the data obtained for the ground states of  $^{30}\text{Al}$  and  $^{28}\text{Al}$  (Figs. 6 and 7), which are both known to be  $3^+$  states. Both of the  $3^+$  predictions reproduce the smooth curve of the data out to  $30^\circ$ , but fail to fit the next maximum. This maximum is possibly the result of two-step contributions to the cross sections, which are discussed later.

The shell model predicts a  $3^+$ , a  $1^+$ , and two  $2^+$  states for the four low lying states, and indeed the data for these levels are too oscillatory to be well fitted by any higher

spin assignments. The first excited state ( $E_x = 0.09$  MeV) is seen to be forward peaked with a possible point of inflection at about  $12^\circ$  and two clear minima ( $20^\circ$  and  $35^\circ$ ). This is best fitted by the  $1^+$  prediction. The next two states ( $E_x = 0.24$  and  $0.42$  MeV) both look very similar, with fewer oscillations, and do not seem to be forward peaked. Assigning these as  $2^+$  states would mean that the shell model correctly predicted the spins and parities of the low lying states, but interchanged the positions of the ground state and the first excited state. (Fig. 3).

Few other levels were extracted at a sufficient range of angles to clearly show their angular distributions. Figure 9 shows fits to these levels. The 2.29 MeV level is seen to be a single smooth curve best fitted by a  $4^+$  prediction, although the  $3^+$  prediction gives good account of all the data other than the isolated forward angle point. The 2.93 MeV level seems best fitted by the lower spin assignments, so a tentative assignment of  $(1,2)^+$  seems reasonable. The cross sections for the 3.23 MeV level are rather oscillatory at large angles but are less so at forward angles—a  $2^+$  assignment is therefore preferred for this level and does seem to fit the data rather well. Of the new levels found by this work, the lower one (4.98 MeV) looks to be a very good candidate for a  $4^+$  state, whereas the higher (5.08 MeV) looks like a  $2^+$ , particularly a  $d_{5/2}^{-1} \times d_{3/2} 2^+$  state, apart from a phase shift. It should be

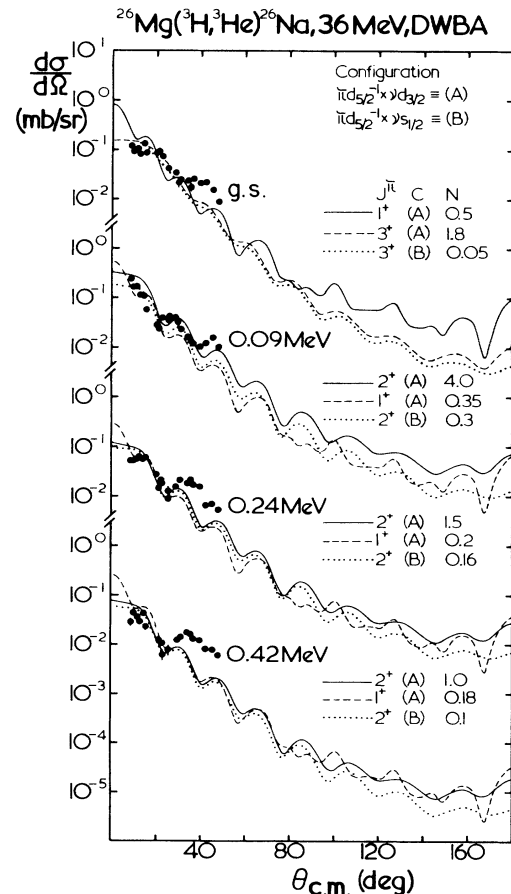


FIG. 8. Direct charge exchange fits for the reaction  $^{26}\text{Mg}(^3\text{H}, ^3\text{He})^{26}\text{Na}$ .

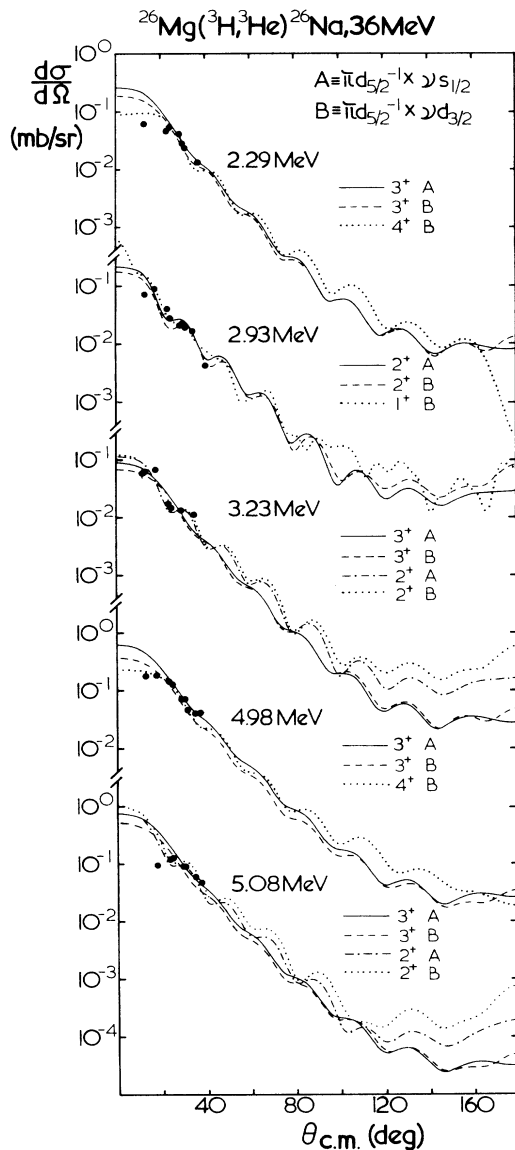


FIG. 9. Direct charge exchange fits for the reaction  $^{26}\text{Mg}(^3\text{H},^3\text{He})^{26}\text{Na}$ .

noted that a phase shift between data and theory has been noticeable in many charge exchange works.

**MICROSCOPIC CHARGE EXCHANGE FITS TO THE  $^{16}\text{O}(^3\text{H},^3\text{He})^{16}\text{N}$  DATA**

Although very little data were collected for the  $^{16}\text{O}(^3\text{H},^3\text{He})^{16}\text{N}$  reaction, it was considered to be worth

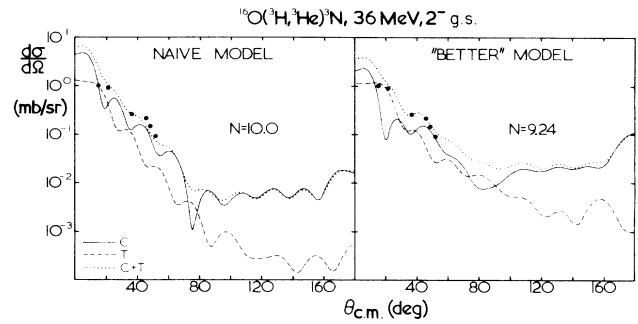


FIG. 10. Direct charge exchange fits for the reaction  $^{16}\text{O}(^3\text{H},^3\text{He})^{16}\text{N}$ .

analyzing because there are some recent papers<sup>9,26</sup> which investigated the reaction  $^{16}\text{O}(^7\text{Li},^7\text{Be})^{16}\text{N}$ , allowing interesting comparisons. The  $^{16}\text{O}(^3\text{H},^3\text{He})^{16}\text{N}$  reaction is ideal for investigating the reaction mechanisms involved because the structure of all the nuclei involved is well known. The spectroscopic amplitudes required are therefore well determined from theory and a wealth of light ion measurements. The  $(^3\text{H},^3\text{He})$  reaction has the advantage over the  $(^7\text{Li},^7\text{Be})$  reaction of having a simpler projectile and ejectile system with no excited states. The use of zero-range approximations are not generally valid for  $(^7\text{Li},^7\text{Be})$  reactions because of the non-*s*-state character of the projectile and ejectile but have been shown to be adequate for the  $(^3\text{H},^3\text{He})$  case.

Figure 10 shows how the microscopic charge exchange predictions compare with the data for the  $2^-$  ground state of  $^{16}\text{N}$ . Two models are employed. The first can be called the "naive model"—this assumes pure particle-hole configurations with the spectroscopic factors calculated accordingly. The second model is more realistic; it uses the same shell model description and spectroscopic amplitudes as Refs. 9 and 26. Table III shows the spectroscopic amplitudes used in these calculations. Comparing the fits obtained from the two models shows that there are some important differences. With the more realistic model the central contribution is reduced by 50% at forward angles and is more oscillatory. Both contributions fall off more rapidly with angle than the data and there is less structure to the angular distribution in the naive model. The fit obtained with the more realistic model passes through all but the first data point if normalized by 9.2. This compares with a normalization of 2.2 found by Cook *et al.*<sup>8</sup> Clarke and Cook<sup>32</sup> show that the Cook *et al.* underestimation of the data was due to the neglect of some high-spin-transfer form factors; they show that including all possible form factors yields predictions slightly overestimating the data. In this present work only two sets of

TABLE III. Spectroscopic amplitudes for  $^{16}\text{O}$  to  $^{16}\text{N}$  (better model).

| Transition | <i>J</i> | $1d_{3/2}$ | $1d_{5/2}$      | $1d_{5/2}$ | $1d_{3/2}$      | $2s_{1/2}$      |
|------------|----------|------------|-----------------|------------|-----------------|-----------------|
|            |          | $1p_{3/2}$ | $1p_{3/2}^{-1}$ | $1p_{3/2}$ | $1p_{1/2}^{-1}$ | $1p_{3/2}^{-1}$ |
| $0^+-2^-$  | 2        | 0.087      | 1.515           | 0.286      | -0.028          | 0.057           |
| $0^+-3^-$  | 3        | 0.007      | 1.294           | -0.199     | 0               | 0               |
| $0^+-4^-$  | 4        | 0          | 0               | 1.155      | 0               | 0               |



form factors are possible, those with  $lsj=112$  and  $lsj=312$ . It has been seen that the 112 case is totally dominated by the central term, while the 312 case is dominated by the tensor interaction.<sup>21</sup> The net effect of this is to have two strong terms out of phase, producing a somewhat featureless angular distribution.

#### DISCUSSION OF THE DIRECT CHARGE EXCHANGE FITS

To be useful as a spectroscopic tool, one particular assumption of spin and parity (the correct one) should yield a far better fit to the data than any other possibility. In the case of the  $^{30}\text{Si}(^3\text{H},^3\text{He})^{30}\text{Al}$  reaction this has not been the case. It seems likely that the assumption in these calculations of pure particle-hole configurations is sufficiently far from the truth in the case of  $^{30}\text{Al}$  to invalidate the calculations. Both  $^{26}\text{Na}$  and  $^{28}\text{Al}$  have more simple shell model configurations (one neutron outside the  $d_{5/2}$  shell compared to three in  $^{30}\text{Al}$ ), and so the assumption is better. The effects of a better shell model of the target and residual have been shown in the case of  $^{16}\text{N}$ . The improved shell model gave predictions with more angular structure and in better agreement with the data.

The angular distributions of the first four states in  $^{26}\text{Na}$  excited by the  $(^3\text{H},^3\text{He})$  reaction have been shown to have sufficient angular structure to allow the assignment of spin parities to be made with some confidence. The assignments for the three low lying excited states are new and demonstrate the potential usefulness of the charge exchange process as a source of information about neutron rich nuclei. The assignments of higher states are more doubtful, although tentative proposals can be forwarded. It is probable that some of the peaks seen in this region correspond to more than one level. Higher resolution work is required to check this feature and to give useful angular distributions. More forward angle data would also help in the assignment of spins since the cross sections expected for  $1^+$  and  $2^+$  states are most differentiated forward of  $10^\circ$ .

The normalizations between the data and the predictions are a problem. In the pure particle-hole model employed, the normalizations would be expected to be less than 1 for most levels since the prediction is for all the configuration's strength, not allowing for the splitting of levels by residual interactions. However, if the model were good and the M3Y strengths reasonable, then the sum of the normalizations over all members of a particular configuration would be unity. To test this fully would require all components of the strength to be identified and extracted accurately, which clearly has not yet been achieved in any experiments. More cause to worry still is that if this simple interpretation of the normalizations is correct, then the same normalizations should be obtained for the  $(^3\text{H},^3\text{He})$  and  $(^7\text{Li},^7\text{Be})$  reactions. Since this is not the case, either the model is very wrong and we are not fitting the direct charge exchange reaction correctly, or the reaction mechanism is more complicated, with two step processes making a significant contribution to the cross section.

#### TWO STEP PROCESSES—INTRODUCTION

It has been shown that direct charge exchange using microscopic form factors often fails to give a particularly good account of the angular distributions. In the following sections two step processes are investigated, which may be expected to make a significant contribution to the reaction cross section.

For a two step process to be important, each step must have a cross section large compared to the direct term. For charge exchange reactions the most important contributions would be expected to be the sequential one-nucleon transfers. Figure 11 shows a coupling diagram including the two possible routes for the  $^{30}\text{Si}(^3\text{H},^3\text{He})^{30}\text{Al}$  reaction:  $^{30}\text{Si}(^3\text{H},^4\text{He})^{29}\text{Al}(^4\text{He},^3\text{He})^{30}\text{Al}$ , proton pickup followed by neutron stripping; and  $^{30}\text{Si}(^3\text{H},^2\text{H})^{31}\text{Si}(^2\text{H},^3\text{He})^{30}\text{Al}$ , neutron stripping followed by proton pickup. The reverse of these routes has been shown to be important in the analysis of  $^{48}\text{Ca}(^3\text{He},^3\text{H})^{48}\text{Sc}$  cross sections and analyzing powers.<sup>26</sup>

When performing these calculations the spectroscopic factors for the first step were obtained from the analysis of the one-nucleon transfer data taken during the experiment.<sup>20</sup> For the second step, however, there was no suitable data taken from this experiment, so it is necessary to use more indirect means. The values of the spectroscopic factors must be taken from the literature when available, or "reasonable" values guessed when no direct measurement is known. Since the spectroscopic factors measured for the first step agreed fairly well with the values given by Cole *et al.*,<sup>27</sup> it seems reasonable to use this paper as a source of the missing spectroscopic factors.

The next question to consider is what levels in the intermediate residual nucleus are important, i.e., what levels do the two step processes feed through? One simple guideline is to assume that the one nucleon transfers should only involve the nucleons that change in the charge exchange reaction. For instance, in the case of  $^{30}\text{Si}(^3\text{H},^3\text{He})^{30}\text{Al}$  a  $d_{5/2}$  proton is replaced by a  $d_{3/2}$  or  $2s_{1/2}$  neutron. Thus, for the proton pickup stage, in which a proton is removed from the target, only the removal of a  $d_{5/2}$  proton need be considered. Another guideline would be to say that the more strongly excited states

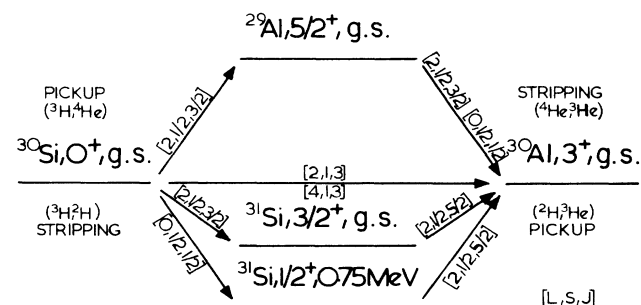


FIG. 11. Coupling diagram for coupled-channels Born approximation (CCBA) calculations.

in the intermediate residual nuclei would make the most significant contributions, so only these need investigating at first.

### TWO STEP CONTRIBUTIONS TO THE $^{30}\text{Si}(^3\text{H},^3\text{He})^{30}\text{Al}$ REACTION

From shell model considerations it can be seen that the proton actively involved in the reaction  $^{30}\text{Si}(^3\text{H},^3\text{He})^{30}\text{Al}$  is almost certainly a  $d_{5/2}$  proton. Thus, for the proton pick-up step in the sequential processes, it seems reasonable to only consider this possibility. Confirmation of this is obtained by looking at the spectra obtained for the reactions  $^{30}\text{Si}(^3\text{H},^4\text{He})^{29}\text{Al}$  and  $^{28}\text{Si}(^3\text{H},^4\text{He})^{27}\text{Al}$ ; in both cases the  $\frac{5}{2}^+$  states in the residual nuclei are most strongly excited.

For the neutron stripping step it is possible for a  $2s_{1/2}$  or  $d_{3/2}$  neutron to be involved. The  $^{30}\text{Si}(^3\text{H},^2\text{H})^{31}\text{Si}$  spectra showed that there are many levels of comparable strength which may be expected to play an important role in determining the final cross section.

For the second step of the sequential transfers, the spectroscopic factors must be obtained indirectly. No spectroscopic factors could be found for  $^{30}\text{Al}$ ; there have been no experimental measurements, so shell model papers tend to overlook this nucleus. For the neutron stripping from  $^{29}\text{Al}$  to  $^{30}\text{Al}$  the spectroscopic factors used were those for neutron stripping from  $^{30}\text{Si}$  to  $^{31}\text{Si}$ , the justification being that from the neutron's point of view the two reactions are entirely analogous, assuming that the neutron and proton shells in nuclei are independent. Taking this approach allows the use of the spectroscopic factors measured during the experiment for both steps of the calculation.

For the  $^{30}\text{Si}(^3\text{H},^2\text{H})^{31}\text{Si}(^2\text{H},^3\text{He})^{30}\text{Al}$  route there are several states in the intermediate nucleus that are strongly excited which should be considered. The second step of this process can be assumed to be purely a  $d_{5/2}$  transfer. Figure 12 (top) shows the predictions for the  $3^+$  ground state of  $^{30}\text{Al}$  for feeding through the first four states of  $^{31}\text{Si}$  and the effect of including all these routes with the same phase. It can be seen that the major contributions come from the  $\frac{3}{2}^+$  g.s. and the  $\frac{1}{2}^+$  level at 0.75 MeV. The  $\frac{5}{2}^+$  1.69 MeV and  $\frac{3}{2}^+$  2.3 MeV levels produce cross sections of similar shape to the ground state route, but about an order of magnitude lower. It seems reasonable either to ignore these levels in future or to approximate their effects by increasing the strength of the included states. This is necessary to prevent the calculations becoming too extensive for the existing computer codes and will only have a slight effect on the final predictions. The solid line in this figure shows the effect of including all four routes in the same calculation, all, in this case, with the same phase. It can be seen that the predictions reproduce the shape of the data fairly well but overestimate the magnitude by a factor of about 2. The calculations were shown to be sensitive to the relative signs (phases) of the different couplings, different combinations making up to a factor of 5 difference in cross section. The shape of the distribution was less sensitive to these phases.

For the  $^{29}\text{Al}(^4\text{He},^3\text{He})^{30}\text{Al}$  step it is possible to transfer a  $s_{1/2}$  or  $d_{3/2}$  neutron. Figure 12 (middle) shows

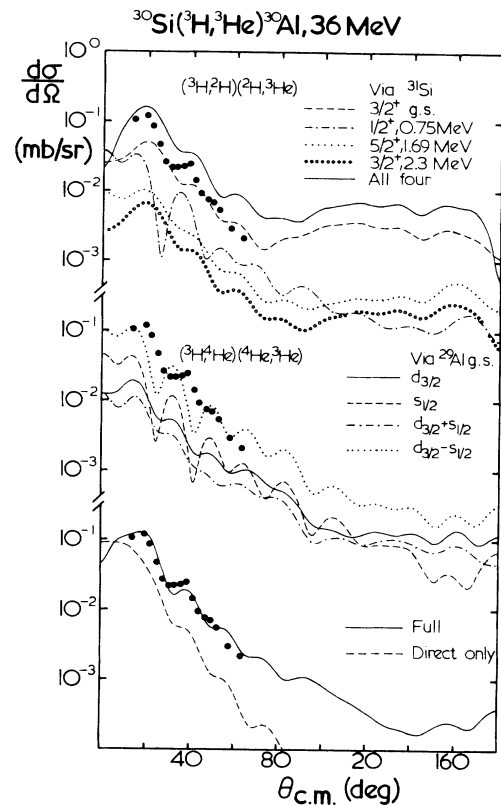


FIG. 12. Two step contributions and full predictions for  $^{30}\text{Si}(^3\text{H},^3\text{He})^{30}\text{Al}$ .

the predictions obtained for the reaction  $^{30}\text{Si}(^3\text{H},^4\text{He})^{29}\text{Al}(^4\text{He},^3\text{He})^{30}\text{Al}$ ; when this step is (a)  $d_{3/2}$  only, (b)  $s_{1/2}$  only, (c)  $d_{3/2}$  and  $s_{1/2}$  (same phase), and (d)  $d_{3/2}$  and  $s_{1/2}$  (opposite phases). It can be seen that the  $d_{3/2}$  and  $s_{1/2}$  terms on their own underestimate the data by up to an order of magnitude. The  $s_{1/2}$ -only calculation is too oscillatory, whereas the  $d_{3/2}$  term alone produces a prediction that is too flat. The effect of the relative phase when both terms are included together is very important. When the phases are of like sign the cross section is suppressed and rather flat; when the phases are opposed, however, the cross sections are comparable to the data, very oscillatory and somewhat out of phase. In the latter case the overall slope and magnitude of the data is well reproduced.

The bottom section of this diagram compares the "full" calculation to the direct charge exchange only calculation. It can be seen that the magnitude of the data is well reproduced (in this diagram both fits are unnormalized) and the detail of the distribution is better fitted. This full calculation was shown to be sensitive to the relative signs of the  $d_{3/2}$  and  $s_{1/2}$  terms for the neutron transfer from  $^{29}\text{Al}$ . If the signs were opposed, the magnitude of the data was increased by a factor of 4 and the phase of the oscillations moved out about  $5^\circ$ . Removing the term altogether produced a very flat angular distribution slightly overpredicting the data.

Figure 13 shows the full calculations to the first four excited states of  $^{30}\text{Al}$ . The lowest excited state ( $E_x=0.245$  MeV) was assumed to be a  $1^+$  (solid line) or a  $2^+$  (dashed line with all phases positive; dotted line with  $s_{1/2}$  phases reversed). Generally, the best fit is obtained assuming a  $1^+$  state; this prediction is the most in phase of the three and reproduces the overall slope better than the other two. An assignment of  $1^+$  does not agree with the shell model predictions.

The second excited state ( $E_x=0.69$  MeV) is known to be a  $1^+$  state. The prediction for this level based on a "full" calculation does reproduce the general features of the distribution, but it is approximately  $8^\circ$  out of phase.

The third excited state observed in this experiment ( $E_x=1.12$  MeV) had previously been assigned a spin of 2, 3, or 4. Of the predictions, the  $1^+$  clearly falls off too rapidly with angle and the  $4^+$  not rapidly enough. The  $2^+$  prediction is too oscillatory, out of phase, and fails to approach the backward angle points. The  $3^+$  fit seems considerably better than any of the others. It reproduces the overall slope of the data and, to a certain extent, the features of the angular distribution. An assignment of  $3^+$ , favored by these fits, agrees with the shell model predictions of this level.

The  $4^+$  level at 1.25 MeV is well fitted out to  $35^\circ$ ,

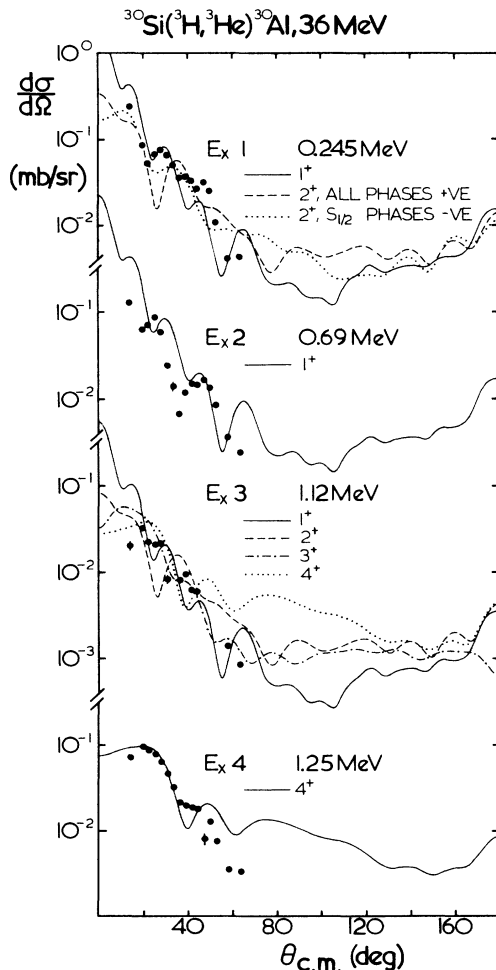


FIG. 13. CCBA calculations for  $^{30}\text{Si}(^3\text{H}, ^3\text{He})^{30}\text{Al}$ .

beyond which the prediction is too oscillatory and overpredicts the data. This may, in fact, indicate that the two step processes have been overestimated in these calculations.

#### TWO STEP CONTRIBUTIONS TO THE $^{28}\text{Si}(^3\text{H}, ^3\text{He})^{28}\text{Al}$ REACTION

Figure 14 shows the various components of the full calculation for the reaction  $^{28}\text{Si}(^3\text{H}, ^3\text{He})^{28}\text{Al}$  to the  $3^+$  ground state. The route via the ground state on  $^{27}\text{Al}$  produces a very oscillatory prediction if a  $2s_{1/2}$  transfer is assumed and a less oscillatory prediction for a  $d_{3/2}$  transfer. In both cases the data are underestimated by between 10 and 2 at forward angles. For the pickup stripping three strong states in  $^{29}\text{Si}$  were considered as possible routes. These all give large and oscillatory predictions with the routes via the excited states of  $^{29}\text{Al}$  overestimating the backward angle data. The full calculation is shown for pure  $d_{5/2} \times d_{3/2}$  and pure  $d_{5/2} \times s_{1/2}$  configurations. Both of these exhibit some features in agreement with the data, but neither fits the overall slope of the data particularly well.

The fits to the first excited state (1.01 MeV  $3^+$ ) (Fig. 15) are not particularly successful; all of the detail of the angular distribution has been washed out, whereas the data display clear angular structure. This clearly indicates that the two step processes have not been included correctly. The fits to the  $1^+$  states are quite successful, except for the usual phase shift problem.

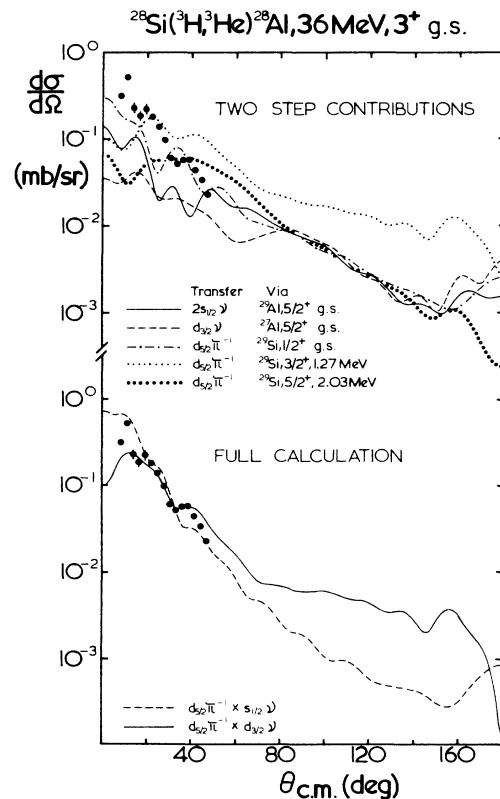


FIG. 14. Two step contributions and full predictions for  $^{28}\text{Si}(^3\text{H}, ^3\text{He})^{28}\text{Al}$ .

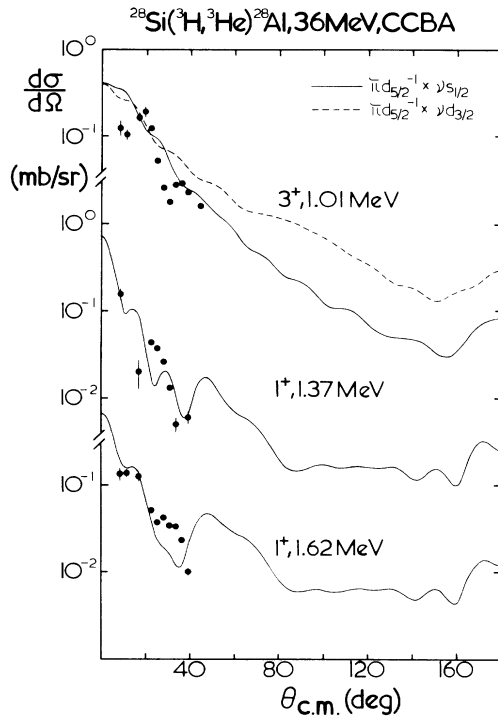


FIG. 15. CCBA calculations for  $^{28}\text{Si}(^3\text{H},^3\text{He})^{28}\text{Al}$ .

**TWO STEP CONTRIBUTIONS TO THE  $^{26}\text{Mg}(^3\text{H},^3\text{He})^{26}\text{Na}$  REACTION**

Figure 16 shows the predictions obtained for the two step excitation of the  $3^+$  ground state of  $^{26}\text{Na}$ . In these calculations the optical model parameters and spectroscopic factors for the first step were those used in fitting the elastic and one-nucleon transfer data obtained during the experiment. The second step spectroscopic factors were taken to be the same because no better values could be found in the literature. Thus the spectroscopic factor used for neutron stripping from  $^{25}\text{Na}$  to  $^{26}\text{Na}$  was that measured for neutron stripping from  $^{26}\text{Mg}$  to  $^{27}\text{Mg}$ . Both the  $\frac{1}{2}^+$  ground state and  $\frac{3}{2}^+$  0.9846 MeV level in  $^{27}\text{Mg}$  were considered as possible routes, whereas only the dominant  $\frac{5}{2}^+$  ground state in  $^{25}\text{Na}$  was included. Both of the stripping-pickup routes via  $^{27}\text{Mg}$  produced oscillatory predictions about a factor of 5 too weak. The pickup-stripping route was of comparable magnitude but less oscillatory, in better agreement with the data. The combination of all three routes with the same phase produced a fit with a very good shape, but a factor of 4 too weak.

Figure 16 (lower) shows the effects of including the direct processes with the normalization found for the direct process alone (solid line). It can be seen that the general shape of the distribution is quite well fitted, but the prediction falls off too rapidly. The effects of doubling the two step strengths (dashed line), then reducing the direct strength still further (dotted line), are also shown in this figure. This shows that a better fit can be obtained by adjusting the strengths of the various contri-

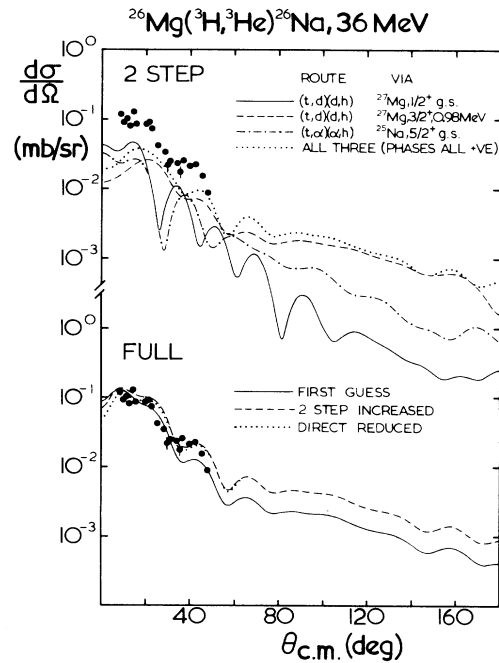


FIG. 16. Two step contributions and full predictions for  $^{26}\text{Mg}(^3\text{H},^3\text{He})^{26}\text{Na}$ .

butions. This may be considered to be a valid process since the strengths were initially “guessed” anyway; on the other hand, there is already a large number of parameters in the model. As has often been noted in this work in others, there is a definite phase shift between the data and the predictions; in this case the difference is about  $5^\circ$ . On the whole, though, the fit is very successful.

Figure 17 shows the full calculations for the first three

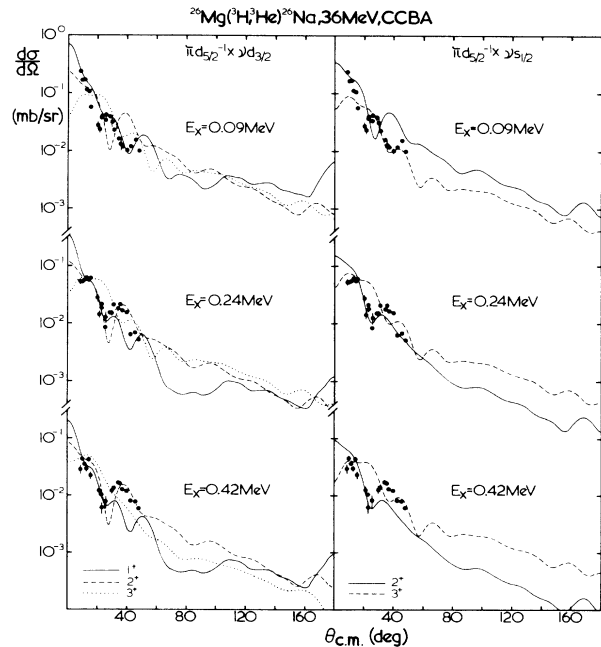


FIG. 17. CCBA calculations for  $^{26}\text{Mg}(^3\text{H},^3\text{He})^{26}\text{Na}$ .

excited states of  $^{26}\text{Na}$ . The calculations have been performed in a pure  $d_{5/2} \times s_{1/2}$  configuration (right) and a pure  $d_{5/2} \times d_{3/2}$  one (left). It can be seen that for the first excited state ( $E_x = 0.09$  MeV) the  $1^+$  state would be the most successful, except for the fact that the first minimum has been filled in. This could indicate that the two step processes have been overestimated or included with the incorrect phase. For both the other states (0.24 and 0.42 MeV) the  $2^+$  predictions are clearly the better of all the alternatives. This reinforces the spin parity assignments made on the basis of the direct charge exchange processes. In both cases the  $d_{5/2} \times d_{3/2}$  configuration gives the best fit to the second maximum in the angular distribution. It is interesting to note that the  $2^+$  prediction is now forward peaked, but not to the same extent as the  $1^+$  prediction.

This section has shown that good fits to the data can be obtained if the relative strengths of the two step processes are varied suitably. Whether this is generally true or if this case was fortuitous will be the subject of later investigation. The spin parity assignments made for the low lying states of  $^{26}\text{Na}$  have been shown to be the ones that would be chosen from the results of full calculations as well as from the direct calculations; thus these assignments are confirmed.

### CONCLUSIONS

The aim of this work had been to investigate the potential usefulness of the charge exchange reaction ( $^3\text{H}, ^3\text{He}$ ) in investigating neutron rich nuclei. It has been demonstrated that the mass of some nuclei can be measured more accurately than before, that previously unknown energy levels can be measured, and that spin and parities can be assigned to these levels.

The ground state mass of  $^{30}\text{Al}$  has been measured to an accuracy of 15 keV, halving the uncertainty of the previous best measurement by Ajzenberg-Selove and Igo.<sup>1</sup> Energy levels up to an excitation of 6 MeV have been detected and measured at a range of angles. Some of these levels were previously unknown, whereas others confirm previously unpublished levels.<sup>10</sup>

A few more levels have been detected in  $^{26}\text{Na}$ , but because of the reduced time spent investigating these nuclei and, therefore, the reduced angular distributions and poorer statistics, some of these observations are considered to be tentative rather than firm.

Calculations of charge exchange cross sections based on microscopic form factors have been investigated. The ( $^3\text{H}, ^3\text{He}$ ) reaction is considered to have advantages over

( $^7\text{Li}, ^7\text{Be}$ ) because of the relative simplicity of the projectile and ejectile and the smaller number of possible  $lsj$  transfer combinations.

It has been confirmed that the tensor components of the interaction are important. These terms are often of equal strength to the central term but out of phase. The resultant cross sections are then less oscillatory than the central-only predictions and agree with the data rather better.

The magnitude of the predicted cross section was shown to be insensitive to the form of the imaginary potentials used in the entrance and exit channels, but sensitive to the real volume integral of the potentials. This sensitivity had not been previously reported.

Little in the way of new spin and parity information about  $^{30}\text{Al}$  was obtained. The first excited state looks more like a  $1^+$  state than the other possibility, a  $2^+$ . The third excited state seen by this work seems to be a good candidate for a  $3^+$  state.

The first four levels of  $^{26}\text{Na}$  were assigned as  $3^+$ ,  $1^+$ ,  $2^+$ , and  $2^+$ , respectively. Only the first state had previously been assigned by gamma and beta decay work. This clearly demonstrates the usefulness of this reaction.

The two step contributions to the cross sections were investigated and it was shown that both stripping pickup and pickup stripping could contribute significantly to the cross section. Some of these calculations were very successful at fitting the angular distributions, others less so. The calculations are full of uncertainties about such things as which routes to include, the spectroscopic factors involved, and the relative phases of the different routes. Some of these problems could possibly be cured with the help of shell model calculations.

The normalization between the predictions and the data are very interesting. If the M3Y interaction is well founded, then ideally the normalizations would always be 1. In fact, since the particle and/or hole strength is often fragmented by residual interactions, the normalization would be expected to be less than 1. The sum of the normalizations over all the fragments of a state would approach 1. However, the normalizations obtained for the ( $^3\text{H}, ^3\text{He}$ ) reaction were often different from that obtained for the ( $^7\text{Li}, ^7\text{Be}$ ) reaction. This difference is thought to be due to the different strengths of the two step processes. Since it was shown that these processes can, in the case of ( $^3\text{H}, ^3\text{He}$ ), account for most of the cross section on their own, this assumption seems to be reasonable. This finding greatly complicates the use of charge exchange reactions either as a spectroscopic tool or for investigation of the effective nucleon-nucleon interaction; regardless, further investigation does seem necessary.

\*Deceased.

<sup>1</sup>F. Ajzenberg-Selove and G. Igo, Phys. Rev. **188**, 1813 (1969).

<sup>2</sup>F. Ajzenberg-Selove, E. R. Flynn, S. Orbesen, and J. W. Sunier, Phys. Rev. D **15**, 1 (1977).

<sup>3</sup>F. Ajzenberg-Selove, E. R. Flynn, D. L. Hanson, and S. Orbesen, Phys. Rev. C **19**, 1742 (1979).

<sup>4</sup>F. Ajzenberg-Selove, E. R. Flynn, D. L. Hanson, and S. Or-

besen, Phys. Rev. C **19**, 2068 (1979).

<sup>5</sup>C. Detraz, D. Guillemaud, G. Huber, R. Klapisch, M. Langevin, F. Naulin, C. Thibault, L. C. Carraz, and F. Touchard, Phys. Rev. C **19**, 164 (1979).

<sup>6</sup>R. L. Kozub, C. B. Chitwood, D. J. Fields, C. J. Lister, J. W. Olness, and E. K. Warburton, Phys. Rev. C **28**, 2343 (1983).

<sup>7</sup>E. R. Flynn and J. D. Garrett, Phys. Rev. C **9**, 210 (1974).

- <sup>8</sup>J. Cook, K. W. Kemper, P. V. Drumn, L. K. Fifield, and M. A. C. Hotchkis, *Phys. Rev. C* **30**, 1538 (1984).
- <sup>9</sup>J. Bang, F. A. Goncharov, and G. S. Kasacha, *Nucl. Phys. A* **429**, 330 (1984).
- <sup>10</sup>A. C. Dodd, Ph.D. thesis, University of London, 1985.
- <sup>11</sup>A. C. Dodd, N. M. Clarke, J. Coopersmith, R. J. Griffiths, K. I. Pearce, B. Stanley, and J. Cook, *J. Phys. G* **11**, 1035 (1985).
- <sup>12</sup>E. R. Flynn, J. Sherman, and N. Stein, *Phys. Rev. Lett.* **32**, 846 (1974).
- <sup>13</sup>F. Ajzenberg-Selove, R. E. Brown, E. R. Flynn, and J. W. Sunier, *Phys. Rev. C* **31**, 777 (1985).
- <sup>14</sup>F. Ajzenberg-Selove, R. E. Brown, E. R. Flynn, and J. W. Sunier, *Phys. Rev. C* **32**, 756 (1985).
- <sup>15</sup>R. Middleton, C. T. Adams, and R. V. Kollarits, *Nucl. Instrum. Methods* **151**, 41 (1978).
- <sup>16</sup>J. S. Lilley, *Phys. Scr.* **25**, 435 (1982).
- <sup>17</sup>Scattering chamber working party of the National Science Foundation's user committee, Daresbury Report, DL/NSF/TM 35, 1978.
- <sup>18</sup>J. B. A. England, M. M. Przybylski, and G. Salvini, Daresbury Report DL/CSE/TM 14, 1981.
- <sup>19</sup>K. I. Pearce, N. M. Clarke, R. J. Griffiths, P. J. Simmonds, D. Barker, J. B. A. England, M. C. Mannion, and C. A. Ogilvie, *J. Phys. G* **12**, 979 (1986).
- <sup>20</sup>K. I. Pearce, N. M. Clarke, R. J. Griffiths, P. J. Simmonds, D. Barker, J. B. A. England, M. C. Mannion, and C. A. Ogilvie, *Nucl. Phys.* (to be published).
- <sup>21</sup>K. I. Pearce, Ph.D. thesis, University of London, 1986.
- <sup>22</sup>P. M. Endt. and V. Van Der Leun, *Nucl. Phys. A* **310**, 1 (1978).
- <sup>23</sup>B. H. Wildenthal, *Prog. Part Nucl. Phys.* **11**, 5 (1984).
- <sup>24</sup>N. M. Clarke, CHEX2, King's College, 1982 (unpublished).
- <sup>25</sup>J. R. Comfort, CHUCK, King's College version.
- <sup>26</sup>N. M. Clarke, *J. Phys. G* **10**, 917 (1984).
- <sup>27</sup>B. J. Cole, A. Watt, and R. R. Whitehead, *J. Phys. G* **2**, 501 (1976).
- <sup>28</sup>W. W. Daenick, J. D. Childs, and Z. Vrceli, *Phys. Rev. C* **21**, 2253 (1980).
- <sup>29</sup>C. B. Fulmer, G. Mariolopoulous, G. Bagieu, A. J. Cole, R. de Swiniarski, and D. H. Koang, *Phys. Rev. C* **18**, 621 (1978).
- <sup>30</sup>R. A. McCulloch, Ph.D. thesis, University of London, 1982.
- <sup>31</sup>A. M. Shahabuddin Meah, Ph.D. thesis, University of London, 1973.
- <sup>32</sup>N. M. Clarke and J. Cook, *Nucl. Phys. A* **458**, 137 (1986).